Research Square

Preprints are preliminary reports that have not undergone peer review.
They should not be considered conclusive, used to inform clinical practice,
or referenced by the media as validated information.

Tissue-dependent detection of somatic variants in vascular malformations with segmental overgrowth: a single-center retrospective multi-tissue study

Minami Tamagake
Tohoku University
Tetsuya Niihori
Tohoku University
Nariaki Takamura
Tohoku University
Ayano Suzuki
ayanojai@gmail.com
Tohoku University
Chieko Miura
Tohoku University
Yoko Aoki
Tohoku University
Yoshimichi Imai
Tohoku University

Research Article

Keywords: somatic mosaicism, vascular malformation, segmental overgrowth, PIK3CA-related overgrowth spectrum, Klippel-Trenaunay syndrome, tissue sampling, molecular diagnosis

Posted Date: November 24th, 2026

DOI: https://doi.org/10.21203/rs.3.rs-11448149/v1

License: This work is licensed under a Creative Commons Attribution 4.0 International License.
Read Full License

Additional Declarations: No competing interests reported.

Abstract

Background

Somatic mosaic variants underlying vascular malformations and segmental overgrowth are often confined to affected tissues and may be present at low variant allele fractions (VAFs), making molecular diagnosis highly dependent on specimen selection. Tissue biopsy, however, can carry substantial risks, including bleeding, lymphatic leakage, and wound complications. This study evaluated tissue-specific patterns of somatic variant detection to inform the selection of diagnostically useful and safer sampling sites.

Results

We retrospectively analyzed 14 patients with segmental overgrowth and vascular malformations using high-depth targeted next-generation sequencing of multiple affected tissues. Pathogenic somatic variants were identified in 9 of 14 patients (64.3%). Among 11 patients with Klippel-Trenaunay syndrome (KTS), *PIK3CA* variants were detected in 8 patients (72.7%); 6 of 6 patients with the capillary-lymphatic-venous malformation phenotype and 2 of 5 with the capillary-venous malformation phenotype (P = 0.061). In *PIK3CA*-positive KTS, the same patient-specific variant was detected in all evaluable overgrown skin/subcutaneous tissue samples (4/4; VAF 7.0–13.0%) and capillary malformation samples (5/5; VAF 3.0–20.0%), whereas it was not detected in any evaluable venous malformation samples (0/3), despite detection in other tissues from the same patients. Neither of two patients with venous malformations and overgrowth had detectable variants in the analyzed tissues. In one patient with a high-flow lesion, *KRAS* c.35G > T (p.Gly12Val) was detected in both overgrowth tissue (VAF 9%) and a nodular vascular lesion (VAF 7%) without biopsy of the high-flow arteriovenous shunt itself.

Conclusions

Somatic variant detection in vascular anomalies with overgrowth showed tissue-dependent patterns that appeared to differ according to the underlying disease and molecular background. These findings support selecting biopsy sites by considering the expected tissue distribution of the causal variant together with procedural safety, rather than applying a uniform sampling strategy to all somatic mosaic vascular anomalies.

Clinical Trial Registration

Not applicable.

Background

The classification and management of vascular anomalies have changed substantially with the clinical implementation of molecular genetics. In the 2025 International Society for the Study of Vascular Anomalies (ISSVA) classification, vascular malformations are classified not only according to clinical and imaging features but also according to their underlying somatic genetic variants[1], and the emergence of molecularly targeted therapies has increased the importance of accurate genetic diagnosis. This paradigm shift has had a particularly marked impact on *PIK3CA*-related overgrowth spectrum (PROS), a group of non-neoplastic disorders caused by somatic gain-of-function variants in *PIK3CA* that arise postzygotically during embryonic development[2]. *PIK3CA* encodes p110alpha, the catalytic subunit of class I PI3K, and activating variants lead to constitutive activation of the downstream PI3K-AKT-mTOR signaling pathway[3]. This promotes excessive cellular proliferation, hypertrophy, and survival, resulting in tissue overgrowth and structural abnormalities.

The clinical phenotype of PROS is highly heterogeneous and varies according to the affected embryonic lineage, predominantly mesodermal and ectodermal tissues, and the developmental stage at which the variant arises[4]. Representative disease entities include Klippel-Trenaunay syndrome (KTS), CLOVES syndrome, megalencephaly-capillary malformation syndrome (MCAP), and localized adipose and connective-tissue overgrowth [5]. Clinical manifestations include segmental and asymmetric overgrowth of the limbs or trunk, involving enlargement of the skin, subcutaneous fat, muscle, and bone, together with various vascular malformations such as capillary, venous, and lymphatic malformations [4, 5]. Functional complications may also include coagulation abnormalities caused by localized intravascular coagulopathy (LIC), chronic pain, epilepsy, and developmental delay associated with central nervous system lesions [6]. Because lesions may be extensive and multisystemic, surgery, endovascular treatment, and laser therapy have limitations. The introduction of PI3K inhibitors and mTOR inhibitors targeting PI3K and its downstream pathway, which are dysregulated by *PIK3CA* variants, has provided clinically transformative therapeutic options for patients with otherwise difficult-to-treat PROS [7, 8], shifting the purpose of genetic testing from academic characterization toward an essential component of precision medicine.

In addition, multiple reports have described patients with overgrowth and vascular malformations that clinically overlap with PROS but harbor somatic variants in other genes [9–13]. Thus, the clinical phenotype does not necessarily predict the genotype, and genetic testing is important for access to appropriate molecularly targeted therapy. Nevertheless, despite the availability of highly sensitive technologies such as next-generation sequencing (NGS), achieving a definitive molecular diagnosis remains a major clinical challenge[2].

A major obstacle is the nature of somatic mosaicism[14]. Pathogenic variants in PROS arise postzygotically, are usually restricted to affected tissues, and may be present at very low variant allele fractions (VAFs), often below the detection limits of conventional assays[15, 16].

Recent international recommendations from VASCERN-VASCA (2024) emphasize the importance of tissue biopsy from affected tissues that characterize the disease [17]; however, there remains no clear

consensus regarding the optimal sampling site in complex, multicomponent lesions. Morin et al. [2] suggested that, when a patient has clear clinical manifestations but no genetic variant is detected in the sampled tissue, resampling a different malformed site in the same patient should be considered. However, compared with biopsy of conventional soft-tissue tumors, tissue sampling from overgrown tissues or vascular malformations in patients with PROS carries higher risks of bleeding and lymphatic leakage, and repeated tissue sampling imposes a substantial burden on patients[18]. In particular, in disorders such as PROS that combine segmental overgrowth with mixed vascular malformations, there are no clear guidelines regarding whether overgrowth tissue or vascular malformation tissue should be sampled, or which lesion should be selected when multiple vascular malformation components coexist. Tissue sampling should minimize patient burden while avoiding false-negative results caused by inappropriate site selection. Nevertheless, when multiple disease-defining lesions coexist, it has not been systematically established which tissue provides the highest sensitivity for variant detection and is therefore the most suitable sampling site for genetic testing [2].

At present, affected tissues containing abnormal vessels are considered a principal source of DNA for somatic variant analysis[17]. High-depth targeted sequencing has the advantage of simultaneously analyzing multiple disease-associated genes with overlapping clinical phenotypes while achieving greater sequencing depth than whole-exome or whole-genome sequencing [2, 19]. Therefore, identifying tissues that are both more likely to yield the causal variant and can be obtained safely remains an important clinical issue when using these analytical approaches.

In this study, we analyzed 14 patients with coexisting segmental overgrowth and vascular malformations. Overgrown skin and subcutaneous tissue, capillary malformations (CMs), venous malformations (VMs), and other affected tissues obtained from the same patients were analyzed using high-depth targeted NGS to investigate tissue-specific patterns of somatic variant detection. The aim of this study was to evaluate appropriate sampling sites for the molecular diagnosis of vascular anomalies caused by somatic mosaicism by considering both diagnostic value and safety in the context of the molecular background of the disease and the tissue distribution of the variant.

Methods

Patients, clinical diagnosis, and ethics:

This was a single-center retrospective observational study of patients who underwent affected-tissue sampling and somatic variant analysis for clinical genetic diagnosis at our institution between April 2023 and March 2026 and who had coexisting overgrowth and vascular malformations.

Overgrowth was defined as a limb-length difference of at least 5 mm in children or at least 10 mm in adults on radiography compared with the contralateral side, or a circumference at least 10% greater than that of the contralateral side on magnetic resonance imaging (MRI)[20, 21]. Vascular malformations were diagnosed according to the ISSVA 2025 classification[1]. Two plastic surgeons specializing in vascular anomalies evaluated the clinical findings, clinical course, and ultrasonographic findings, and

diagnoses were established in conjunction with radiologic assessment of MRI, computed tomography (CT), and angiography when required.

The inclusion criteria were a clinical diagnosis of a vascular malformation based on the ISSVA 2025 classification[1], coexisting segmental overgrowth meeting the criteria described above, and somatic variant analysis using affected tissue. The final cohort comprised 14 patients: 11 with KTS, two with venous malformations accompanied by tissue overgrowth, and one with a high-flow lesion characterized by tissue overgrowth, an arteriovenous shunt, and peripheral venous dilatation.

Informed consent

was obtained from all participants or their legal representatives. The study was approved by the Institutional Review Board of Tohoku University Hospital (No. 2025-1-541), and all procedures were conducted in accordance with the Declaration of Helsinki and its subsequent amendments.

Multi-tissue sampling protocol:

To investigate the tissue distribution of somatic variants, fresh samples of multiple clinically accessible affected tissues were obtained from each patient by surgical biopsy or needle biopsy.

For capillary malformations (CMs), an approximately 1-cm spindle-shaped specimen including the full thickness of the skin and attached subcutaneous adipose tissue was obtained from a geographic red patch within the overgrown region. (Fig. 1 (a),(b),(c))

For overgrown skin and subcutaneous tissue, an approximately 1-cm spindle-shaped specimen containing the full thickness of the skin and subcutaneous adipose tissue was obtained from an overgrown area without a red patch or superficial VM. (Fig. 1 (a),(b),(d)) Alternatively, in patients undergoing debulking surgery, a portion of the resected excess overgrown tissue was submitted for analysis.

For venous malformations (VMs), superficial lesions were sampled as approximately 1-cm specimens containing the full thickness of the skin, subcutaneous tissue, and the vascular lesion. For deep lesions, the lesion was identified under image guidance. Lesions superficial to the superficial fascia were exposed and partially excised (Fig. 1 (e), (f), (g)), whereas lesions deeper than the superficial fascia were sampled by repeated needle biopsy under ultrasonographic and fluoroscopic guidance. (Fig. 1 (h), (i))

In patients with nodular abnormal vascular lesions that did not clearly correspond to an established vascular malformation category, such lesions were also included in the analysis when tissue could be obtained.

The arteriovenous shunt itself, representing the high-flow lesion, was not biopsied because of the risk of bleeding associated with tissue sampling.

DNA extraction and library preparation:

Collected specimens were cut into approximately 5-mm cubes and stored in an ultra-low-temperature freezer at -80 degrees C or below. DNA was extracted within 1 month of collection using the DNeasy Blood & Tissue Kit (QIAGEN). The DNA input used for analysis ranged from 5 to 200 ng.

Targeted next-generation sequencing:

With reference to Nozawa et al. (2020) [22], panel analysis was performed by NGS using the AmpliSeq for Illumina Cancer Hotspot Panel v2 (Illumina, Hayward, CA, USA), which includes *KRAS*, *NRAS*, *HRAS*, *GNAQ*, *GNA11*, *PIK3CA*, *PTEN*, *PTPN11*, and other genes. Sequencing was performed on a MiSeq instrument (Illumina) using 2 x 150-bp paired-end reads. Mean coverage of the target regions exceeded 2,000x. Analysis was performed using VariantStudio Data Analysis Software v3.0 (Illumina).

Bioinformatics analysis

FASTQ data were trimmed using Trim Galore! (v0.6.10, https://www.bioinformatics.babraham.ac.uk/projects/trim_galore/) and mapped to hg19 using BWA (v0.7.9a)[23]. Variant calling was performed using GATK (v4.2.5.0) HaplotypeCaller and Mutect2[24]. Variants were annotated using ANNOVAR[25] and filtered based on population databases, such as gnomAD v2.1.1[26] and HGVD v1.0[27] and clinical genetic databases including ClinVar[28] and HGMD[29]. All identified pathogenic variants were manually inspected using the Integrative Genomics Viewer (IGV)[30].

Statistical analysis:

The primary analysis focused on the detection of somatic variants across different tissue types. Because the number of patients was limited and multiple tissue specimens were obtained from the same patients, variant detection by tissue type was summarized primarily using descriptive statistics, including the number of detected variants divided by the number of evaluable specimens and the corresponding detection rate. Because multiple specimens obtained from the same patient were not independent observations, simple tests comparing independent groups were not performed for variant detection rates across tissue types.

The association between clinical phenotype (capillary-lymphatic-venous malformation [CLVM] and capillary-venous malformation [CVM]) and patient-level *PIK3CA* variant detection in patients with KTS was evaluated exploratorily using Fisher's exact test. All tests were two-sided, and $P < 0.05$ was considered statistically significant. Statistical analyses were performed using JMP Student Edition (version 19.2; JMP Statistical Discovery LLC, Cary, NC, USA). Exact two-sided 95% confidence intervals for binomial proportions were calculated using the Clopper–Pearson method.

Results

Clinical phenotypes and cohort characteristics:

Fourteen patients with vascular malformations associated with overgrowth were enrolled in this study.

According to the ISSVA 2025 classification, the cohort was divided into three groups: KTS (n = 11), venous malformations accompanied by tissue overgrowth (VM group, n = 2), and a high-flow lesion with overgrowth (FF group, n = 1). The clinical characteristics of individual patients are summarized in Table 1.

Table 1
Clinical characteristics of the study cohort Klippel–Trenaunay syndrome (n = 11)

Case	Age, y	Sex	Phenotype	Vascular malformations	Overgrowth
KTS1	17	Female	CLVM	Superficial and deep lymphatic malformations, venous malformation, and extensive capillary malformation of the right lower extremity	Soft-tissue overgrowth from the right lumbar region to the toes; leg-length discrepancy; macrodactyly
KTS2	4	Male	CLVM	Superficial and deep lymphatic malformations, venous malformation, and geographic capillary malformation of the right lower extremity	Soft-tissue overgrowth predominantly extending from the right lumbar region to the knee, with milder overgrowth below the knee; leg-length discrepancy.
KTS3	18	Male	CLVM	Capillary malformations of the left lateral chest and lower leg; superficial and deep lymphatic malformations	Soft-tissue overgrowth of the left lateral chest; leg-length discrepancy; macrodactyly
KTS4	4	Female	CLVM	Superficial and deep lymphatic malformations, venous malformation, and capillary malformation of the left buttock and lower extremity	Soft-tissue overgrowth from the left lumbar region to the toes; leg-length discrepancy; macrodactyly
KTS5	12	Female	CLVM	Capillary malformation of the left knee; superficial and deep lymphatic malformations of the left lower extremity; megavein	Soft-tissue overgrowth from the left buttock to the foot; leg-length discrepancy
KTS6	46	Female	CLVM	Capillary malformation of the right lower leg; deep lymphatic malformation; venous malformation	Soft-tissue overgrowth from the right lumbar region to the toes; leg-length discrepancy; macrodactyly
KTS7	5	Female	CVM	Capillary malformations of the right toes and dorsum of the foot; venous malformation of the foot; megavein	Soft-tissue overgrowth of the right foot; leg-length discrepancy
KTS8	10	Female	CVM	Multiple venous malformations and patchy capillary malformation of the right lower extremity	Soft-tissue overgrowth of the right lower extremity; leg-length discrepancy

Case	Age, y	Sex	Phenotype	Vascular malformations	Overgrowth
KTS9	22	Female	CVM	Scattered capillary malformations around the right knee/lower leg and multiple venous malformations from the thigh to lower leg	Soft-tissue overgrowth of the right lower extremity; leg-length discrepancy
KTS10	33	Male	CVM	Capillary malformation of the posterior left thigh and multiple venous malformations of the knee/lower leg	Soft-tissue overgrowth of the left lower leg; leg-length discrepancy
KTS11	28	Female	CVM	Capillary malformation of the right thigh and multiple venous malformations of the lower extremity	Soft-tissue overgrowth of the right lower leg; leg-length discrepancy

Clinical characteristics of the 14 patients with vascular malformations and segmental overgrowth are summarized. The cohort comprised 11 patients with Klippel–Trenaunay syndrome (KTS), two with venous malformations (VMs) and overgrowth, and one with a high-flow lesion and overgrowth. Patients with KTS were classified as having either the capillary–lymphatic–venous malformation (CLVM) or capillary–venous malformation (CVM) phenotype. Age is presented in years. The em dash (—) indicates that no additional findings were reported.

Abbreviations: CLVM, capillary–lymphatic–venous malformation; CVM, capillary–venous malformation; KTS, Klippel–Trenaunay syndrome; VM, venous malformation.

Venous malformation and high-flow groups

Within the KTS group, six patients had a CLVM phenotype and five had a CVM phenotype. Representative cases of the CLVM and CVM phenotypes are shown in Figs. 2 and 3, respectively.

Diagnostic yield of targeted panel analysis:

Detailed specimen-level results, including the analyzed tissue, sampling site, detected somatic variant, and variant allele fraction, are summarized in Table 2. Pathogenic somatic variants were identified in 9 of 14 patients by high-depth targeted sequencing using the targeted gene panel, corresponding to an overall detection rate of 64.3%.

Table 2
Tissue-specific somatic variant analysis by patient Klippel–Trenaunay syndrome

Case	Phenotype/group	Analyzed tissue	Sampling site	Somatic variant	VAF, %
KTS1	CLVM	Overgrown skin/subcutis	Right toes	*PIK3CA* c.1624G > A (p.Glu542Lys)	7.0
KTS2	CLVM	Overgrown skin/subcutis	Right foot	*PIK3CA* c.3140A > G (p.His1047Arg)	7.0
KTS3	CLVM	Capillary malformation	Left anterior chest	*PIK3CA* c.1624G > A (p.Glu542Lys)	15.0
KTS4	CLVM	Overgrown skin/subcutis	Left thigh	*PIK3CA* c.1633G > A (p.Glu545Lys)	13.0
KTS5	CLVM	Capillary malformation	Left knee	*PIK3CA* c.1258T > C (p.Cys420Arg)	5.0
KTS5	CLVM	Overgrown skin/subcutis	Left knee, superficial	*PIK3CA* c.1258T > C (p.Cys420Arg)	7.0
KTS6	CLVM	Capillary malformation	Right lower leg	*PIK3CA* c.3073A > G (p.Thr1025Ala)	20.0
KTS6	CLVM	Venous malformation	Right lower leg, superficial	Not detected	—
KTS7	CVM	Capillary malformation	Dorsum of right foot	Not detected	—
KTS7	CVM	Venous malformation	Right ankle	Not detected	—
KTS8	CVM	Capillary malformation	Right knee	*PIK3CA* c.1258T > C (p.Cys420Arg)	7.0
KTS8	CVM	Venous malformation	Right lower leg	Not detected	—
KTS9	CVM	Capillary malformation	Right lower leg	*PIK3CA* c.1633G > A (p.Glu545Lys)	3.0
KTS9	CVM	Venous malformation	Right knee	Not detected	—
KTS10	CVM	Capillary malformation	Posterior left thigh	Not detected	—
KTS10	CVM	Venous malformation	Left knee	Not detected	—
KTS11	CVM	Capillary malformation	Right thigh	Not detected	—

For each analyzed specimen, the tissue type, anatomical sampling site, detected somatic variant, and variant allele fraction (VAF) are shown. Patients from whom more than one tissue specimen was analyzed appear in multiple rows. “Not detected” indicates that no pathogenic somatic variant was identified in the specimen using the targeted gene panel; it does not exclude variants outside the panel or below its detection threshold. A dash (—) in the VAF column indicates that no VAF is reported because no variant was detected.

Abbreviations: CLVM, capillary–lymphatic–venous malformation; CVM, capillary–venous malformation; VAF, variant allele fraction; VM, venous malformation.

Venous malformation and high-flow groups

In the KTS group, *PIK3CA* variants were identified in 8 of 11 patients (72.7%). *PIK3CA* variants were identified in all six patients with the CLVM phenotype (6/6, 100%) and in two of five patients with the CVM phenotype (2/5, 40%). Although the detection rate was numerically higher in the CLVM group, the difference was not statistically significant (Fisher's exact test, P = 0.061). The detected hotspot variants were p.Glu542Lys (PIK3CA c.1624G > A), p.His1047Arg (PIK3CA c.3140A > G), and p.Glu545Lys (PIK3CA c.1633G > A), and the non-hotspot variants were p.Cys420Arg (PIK3CA c.1258T > C) and p.Thr1025Ala (PIK3CA c.3073A > G). Hotspot variants were detected in five of eight *PIK3CA*-positive patients (62.5%), including four of six patients in the CLVM group (66.7%) and one of two patients in the CVM group (50.0%), with no significant difference. Non-hotspot variants were detected in three of eight patients (37.5%), including two of six patients in the CLVM group (33.3%) and one of two patients in the CVM group (50.0%).

Within-patient tissue-specific variant detection patterns in *PIK3CA*-positive KTS

Among the 11 patients with KTS, eight in whom a *PIK3CA* variant was confirmed in at least one affected tissue were evaluated for tissue-specific variant detection within the same patient. This analysis was a tissue-distribution analysis restricted to patients confirmed to be *PIK3CA*-positive and was not intended to estimate the diagnostic sensitivity of each tissue type. In addition, not all tissue types were obtained from every patient; therefore, the denominators below represent the number of patients in whom each tissue type was actually obtained and evaluable.

Among the four patients in whom overgrown skin and subcutaneous tissue could be analyzed, *PIK3CA* variants were detected in all four (4/4), with VAFs ranging from 7.0% to 13.0%. Similarly, *PIK3CA* variants were detected in all five patients with evaluable CM tissue (5/5), with VAFs ranging from 3.0% to 20.0%.

In contrast, among the three patients in whom VM tissue could be analyzed, the same *PIK3CA* variant was not detected in any VM specimen (0/3), despite confirmation of the variant in another affected tissue from the same patient.

Because the number of patients was small and multiple specimens from the same patient were not independent observations, no formal statistical comparison among tissue types was performed.

Nevertheless, in *PIK3CA*-positive KTS, a within-patient tissue-dependent pattern of variant detection was observed: patient-specific *PIK3CA* variants were consistently detected in overgrown skin/subcutaneous tissue and CM, whereas they were not detected in the evaluable VM specimens. Exact 95% confidence intervals for the patient-level variant detection rates and the descriptive tissue-distribution proportions in *PIK3CA*-positive KTS are summarized in Table 3.

Table 3
Exact 95% confidence intervals for somatic variant detection

Group / specimen	Detection, n/N (%)	Exact 95% CI
Patient-level detection		
Overall cohort	9/14 (64.3%)	35.1–87.2%
KTS	8/11 (72.7%)	39.0–94.0%
CLVM	6/6 (100%)	54.1–100.0%
CVM	2/5 (40.0%)	5.3–85.3%
Tissue distribution among PIK3CA-positive KTS*		
Overgrown skin/subcutis	4/4 (100%)	39.8–100.0%
Capillary malformation	5/5 (100%)	47.8–100.0%
Venous malformation	0/3 (0%)	0.0-70.8%

Detection proportions are presented as n/N (%), with two-sided exact binomial 95% confidence intervals calculated using the Clopper–Pearson method. The overall cohort row represents the proportion of patients with any detected pathogenic somatic variant. The KTS, CLVM, and CVM rows represent patient-level PIK3CA variant detection.

The tissue-specific rows are restricted to patients with PIK3CA-positive KTS; denominators represent the numbers of patients with evaluable tissue of each corresponding type. These conditional tissue-distribution proportions should not be interpreted as estimates of diagnostic sensitivity. The exploratory comparison of patient-level PIK3CA variant detection between the CLVM and CVM phenotypes was performed using a two-sided Fisher's exact test (P = 0.061).

Abbreviations: CI, confidence interval; CLVM, capillary–lymphatic–venous malformation; CM, capillary malformation; CVM, capillary–venous malformation; KTS, Klippel–Trenaunay syndrome; VM, venous malformation.

VM group:

VM1 had multiple venous malformations in the right lower extremity with ipsilateral lower-leg overgrowth, as well as a separate localized venous malformation in the left mandibular region. The characteristic clinical and imaging findings of patient VM1 are shown in Fig. 4. Tissue samples were obtained from the overgrown tissue of the right lower leg, a venous malformation in the right lower leg, and the left mandibular venous malformation; no pathogenic variants were detected in any of these specimens.

Similarly, no pathogenic variants were detected in either the overgrowth tissue or venous malformation tissue obtained from VM2.

FF case:

Patient FF1 presented with an erythematous patch with skin dryness on the lower leg, soft-tissue overgrowth, limb-length discrepancy, and dilated veins. Contrast-enhanced computed tomography (CT) revealed an arteriovenous shunt around the ankle, and a low-flow nodular vascular lesion was observed near the left knee (Fig. 5). Because of the risk of bleeding, the high-flow lesion was not biopsied. Instead, tissue samples were obtained from the overgrown soft tissue of the left lower leg and the nodular vascular lesion near the left knee. No *PIK3CA* variant was detected, whereas the *KRAS* variant, c.35G > T (p.Gly12Val), was identified in both the overgrowth tissue (VAF 9%) and the nodular vascular lesion (VAF 7%).

A patient-by-tissue summary of somatic variant detection and variant allele fractions across the study cohort is provided in Table 4.

Table 4
Tissue-specific somatic variant detection and variant allele fraction by patient

Patient	Phenotype / group	Variant	Overgrown skin/ subcutis	CM	VM	Other vascular lesion
KTS1	CLVM	*PIK3CA* p.Glu542Lys	+ (7%)	—	—	—
KTS2	CLVM	*PIK3CA* p.His1047Arg	+ (7%)	—	—	—
KTS3	CLVM	*PIK3CA* p.Glu542Lys	—	+ (15%)	—	—
KTS4	CLVM	*PIK3CA* p.Glu545Lys	+ (13%)	—	—	—
KTS5	CLVM	*PIK3CA* p.Cys420Arg	+ (7%)	+ (5%)	—	—
KTS6	CLVM	*PIK3CA* p.Thr1025Ala	—	+ (20%)	-	—
KTS7	CVM	Not detected	—	-	-	—
KTS8	CVM	*PIK3CA* p.Cys420Arg	—	+ (7%)	-	—
KTS9	CVM	*PIK3CA* p.Glu545Lys	—	+ (3%)	-	—
KTS10	CVM	Not detected	—	-	-	—
KTS11	CVM	Not detected	—	-	—	—
VM1	VM with overgrowth	Not detected	-	—	– (2 sites)	—
VM2	VM with overgrowth	Not detected	-	—	-	—
FF1	High-flow with overgrowth	*KRAS* p.Gly12Val	+ (9%)	—	—	+ (7%)

Tissue-specific somatic variant detection and variant allele fractions by patient

Each row represents one patient and summarizes the detected pathogenic somatic variant and its distribution across the analyzed tissues. A plus sign (+) indicates variant detection, with the corresponding VAF shown in parentheses; a minus sign (−) indicates that the tissue was analyzed but no pathogenic somatic variant was detected using the targeted panel; an em dash (—) indicates that the corresponding tissue was not analyzed.

For VM1, two anatomically distinct venous malformations (right lower leg and left mandibular region) were analyzed, and neither yielded a detectable pathogenic variant.

For FF1, KRAS p.Gly12Val was detected in overgrown skin/subcutaneous tissue of the left lower leg (VAF 9%) and a nodular vascular lesion near the left knee (VAF 7%); the high-flow arteriovenous shunt itself was not biopsied.

Abbreviations: CLVM, capillary–lymphatic–venous malformation; CM, capillary malformation; CVM, capillary–venous malformation; KTS, Klippel–Trenaunay syndrome; VAF, variant allele fraction; VM, venous malformation.

Discussion

Curative treatment is often difficult for vascular malformations and overgrowth syndromes, including PROS[31], and molecularly targeted therapies such as mTOR inhibitors and PI3K inhibitors have become important therapeutic options [7, 8]. Genetic testing is therefore important not only for diagnosis and classification but also for enabling access to appropriate molecularly targeted therapies [32, 33]. At the same time, these disorders are driven by somatic mosaicism, and sampling of affected tissue carries risks such as bleeding, lymphatic leakage, and wound complications [34]. Thus, determining which of the overgrown tissues or multiple vascular malformations should be selected as a safe specimen with high diagnostic value remains an important clinical issue[2].

A distinctive feature of this study is that we did not compare variant detection rates across tissue types between different patients; instead, we evaluated multiple affected tissues obtained from the same patients using the same analytical platform. In disorders caused by somatic mosaicism, VAF varies according to the causal variant, the developmental timing of the variant, the extent of the lesion, and the degree of mosaicism in each patient. Therefore, interpatient comparisons alone make it difficult to evaluate the effect of tissue type itself on variant detection. Our within-patient comparison partially reduces the influence of these interpatient differences and allows the relationship between specimen selection and variant detection to be assessed.

In recent years, liquid biopsy using cell-free DNA (cfDNA) has attracted attention as a minimally invasive approach to genetic diagnosis. However, the present study does not compete with these emerging approaches; rather, it addresses a distinct clinical question: the optimal sampling site in current tissue-based genetic diagnosis. Although advances in liquid biopsy may reduce the need for tissue biopsy in the future, defining an appropriate sampling strategy when affected tissue is used remains an important issue at present [2, 17].

PIK3CA variants and phenotypic diversity

In disorders caused by somatic mosaicism, differences in the developmental timing of a variant and in the cells and tissues in which it is distributed contribute to phenotypic diversity and complicate

appropriate specimen selection. *PIK3CA* encodes p110alpha, one of the catalytic subunits of class I PI3K[35]. Gain-of-function variants in *PIK3CA* constitutively activate downstream signaling, including mTORC1, thereby promoting cellular hypertrophy and proliferation and resulting in tissue overgrowth[36]. In addition, p110alpha is important for the development of both blood and lymphatic vessels [37, 38], and excessive endothelial-cell proliferation has been shown to produce dilated, dysfunctional vessels [39].

The phenotype of PROS is thought to be determined by multiple factors, including the developmental stage at which the variant arises, the cell type affected, the variant allele fraction, and whether the variant is a hotspot variant [40]. Variants arising early in development may result in extensive phenotypes such as PROS, whereas variants arising later may manifest as localized lesions such as lymphatic or venous malformations [41]. In addition, PROS preferentially affects mesoderm-derived tissues such as adipose tissue, blood vessels, muscle, and bone, as well as some neuroectoderm-derived tissues, whereas endoderm-derived tissues are relatively less affected[3] Thus, differences in developmental timing and tissue/cellular distribution are thought to contribute to the diverse phenotypes produced by a single somatic *PIK3CA* variant[4].

Tissue distribution of *PIK3CA*-mutant cells

Multiple studies have shown that *PIK3CA* variants in lymphatic malformations (LMs) and VMs are predominantly present in lesional endothelial cells[42]. Blesinger et al. (2018) isolated endothelial cells and fibroblasts from patients with LM and detected *PIK3CA* variants in LM endothelial cells[43]. Le Cras et al. (2020) identified *PIK3CA* hotspot variants in endothelial cells isolated from lymphatic and venous malformations in CLVM and demonstrated constitutive AKT phosphorylation, increased proliferation, and resistance to cell death compared with normal endothelial cells [44]. In contrast, Tooming et al. (2025) detected *PIK3CA* variants in cultured fibroblasts derived from the skin of patients with PROS[45]. These findings indicate that *PIK3CA*-mutant cells in PROS may be distributed not only among endothelial cells within vascular malformations but also among stromal cells in the skin and subcutaneous tissue.

Differences in variant detection patterns among tissues observed in this study

In this study, we attempted to include lesional endothelial cells, surrounding connective tissue, skin, and subcutaneous tissue as extensively as possible when sampling vascular malformation tissue. As a result, *PIK3CA* variants were consistently detected in CM and overgrowth tissues in *PIK3CA*-positive KTS, whereas they were not detected in the corresponding VM specimens. Two possible explanations for this finding are that the histologic architecture of VM diluted mutant-cell-derived DNA such that the VAF fell below the detection threshold, and that genes outside the panel other than *PIK3CA* contributed to the lesions.

Possibility of low VAF related to the histologic architecture of VM

Histologically, VMs consist of dilated blood-filled vascular spaces, smooth-muscle layers, and extensive fibrous stroma[46, 47]; therefore, the number of cells contained in an equivalent amount of tissue may be lower than in other affected tissues [48]. If *PIK3CA*-mutant cells are located predominantly in endothelial cells and some stromal cells, mutant DNA extracted from bulk tissue may be diluted by DNA from non-mutant cells, causing the VAF to fall below the detection threshold of the panel used in this study.

Martinez et al. (2026) reported that, although obtaining tissue directly from a VM is useful for molecular diagnosis, percutaneous biopsy carries risks of bleeding and inadequate sampling; they therefore described a transvenous biopsy approach through an outflow vein [18]. This also suggests that both the location and method of VM sampling may influence the success of genetic analysis.

Furthermore, *PIK3CA*-mutant cells may contribute to lesion formation not only through cell-autonomous effects but also by influencing surrounding non-mutant cells through paracrine factors, exosomes, and alterations in the extracellular matrix[3]. Therefore, even among tissues affected by the same *PIK3CA* variant and contributing to the same lesion phenotype, it remains unclear how many mutant cells are present in each tissue, which cells carry the variant, and which cells are affected indirectly. The pattern observed in this study, in which variants were detected in CM and overgrowth tissues but not in VM, may reflect differences in the proportion of mutant cells among tissue types. For VM, further investigation of more appropriate tissue-sampling methods and high-depth analysis targeting genes with a high likelihood of detection, including *PIK3CA*, genes in the RAS pathway, and *TEK*, is required.

Possible involvement of genes outside the panel other than *PIK3CA*

In patients with coexisting overgrowth and vascular malformations, the coexistence of multiple somatic variants has also been reported. Chen et al. reported *PIK3CA* variants in 67 of 82 patients (81.7%) with suspected PROS; among these, six patients also had variants in other genes, and three patients with KTS had variants in *STAMBP*, *MAP2K1*, and *MAP3K3*, respectively, in addition to *PIK3CA* variants [49]. Coexisting *PIK3CA* and *TEK* variants have also been reported in VM[10, 49]. It remains unclear how the presence of mosaic variants involving two or more genes affects the phenotype or how these variants are spatially distributed. Therefore, VMs in which no variant was detected in this study may harbor variants in genes other than *PIK3CA* that were not included in the analytical panel, and additional analysis using a more comprehensive gene panel is warranted.

VM group:

In a review of 300 patients with common venous malformations, *TEK* and *PIK3CA* variants were reported in 41.3% and 26.7% of patients, respectively [50]. This may partly explain the absence of *PIK3CA* variants in the VM group in the present study. *PIK3R1* has also been associated with VM accompanied by overgrowth, although such cases are rare [2], and overgrowth is not a major phenotype of Blue Rubber Bleb Nevus Syndrome, which is characterized by multiple VMs [2]. Overgrowth associated with VM may include secondary changes resulting from increased blood flow, hematoma formation, fibrosis, and

edema caused by venous stasis, and some cases may therefore involve mechanisms different from those underlying overgrowth in PROS.

Accordingly, tissue selection for genetic analysis should be considered differently in KTS and in cases in which VM is the predominant lesion accompanied by overgrowth. In the latter, the VM itself may be an important tissue for analysis, and specimens should be selected according to the molecular background of the disease. Additional cases are needed to validate this concept.

FF case: mosaic RASopathy

In FF1, the known oncogenic variant *KRAS* c.35G > T (p.Gly12Val)[51] was detected, supporting a diagnosis of mosaic RASopathy caused by a postzygotic somatic activating variant in the RAS/MAPK pathway. The clinical spectrum of mosaic RASopathy is broad, ranging from localized lesions to multisystem manifestations resembling germline RASopathies, and may overlap clinically with PROS[2, 52].

Multiple patients presenting with overgrowth and vascular malformations and initially suspected of having PROS have been reported to harbor somatic variants in the RAS/MAPK pathway, including *KRAS* c.35G > T (p.Gly12Val)[53–55], *KRAS* c.35G > A (p.Gly12Asp) [53, 56, 57], *KRAS* c.38G > A (p.Gly13Asp) [56], and *KRAS* c.183A > T (p.Gln61His) [55]. Coexisting *PTPN11* c.1520C > A (p.Thr507Lys) and *FGFR1* c.1632C > A (p.Asn544Lys) variants have also been reported in the same patient[58]. Although high-flow vascular malformations have been proposed as a feature distinguishing these disorders from PROS [2], RAS-pathway variants have also been reported in patients with low-flow vascular malformations and overgrowth, underscoring the phenotypic diversity of mosaic RASopathy.

An additional clinical implication of our case is that the same *KRAS* c.35G > T (p.Gly12Val) variant was detected in multiple affected tissues with different phenotypes without biopsy of the high-flow lesion itself. In mosaic RASopathy, somatic variants in the RAS/MAPK pathway have been reported to occur across multiple tissue lineages, including vascular malformations, segmental overgrowth, capillary malformations, epidermal nevi, and bone lesions [52]. In addition, a causal variant has been detected in overgrown subcutaneous soft tissue in a patient with a mosaic *KRAS* variant and an arteriovenous malformation[55].

Taken together with the present case, these findings suggest that when mosaic RASopathy is suspected in a patient with segmental overgrowth or superficial lesions, a high-flow vascular lesion associated with bleeding risk may not necessarily need to be the first-choice biopsy site; more safely accessible overgrowth tissue or superficial affected tissue may serve as an initial specimen. However, systematic studies comparing the tissue distribution of variants in mosaic RASopathy remain limited, and further investigation is required before this sampling strategy can be generalized.

Overall, these findings suggest that, in vascular anomalies caused by somatic mosaicism, the pattern of variant detection and the tissue with the greatest diagnostic value may differ according to the disease

and its molecular background. Rather than applying a uniform sampling site to all patients, specimen selection should consider the suspected causal gene, the expected tissue distribution of the variant, and the procedural risk of tissue acquisition.

Clinical implications: tissue selection for less invasive molecular diagnosis

In KTS, *PIK3CA* variants were consistently detected in overgrown skin/subcutaneous tissue and CM, whereas they were not detected in corresponding VM tissue. Therefore, when a new tissue sample is required for genetic analysis, superficial CM or overgrown skin/subcutaneous tissue may reasonably be prioritized over VM associated with a risk of bleeding. In contrast, VM may require optimization of both sampling and analytical methods. In the mosaic RASopathy case in this study, the same *KRAS* variant was detected in overgrowth tissue and another affected lesion without direct biopsy of the high-flow lesion, suggesting that more safely accessible affected tissue may be selected as a specimen according to the molecular background. This concept is consistent with the direction of molecular diagnosis reflected in ISSVA 2025[1] and VASCERN-VASCA (2024)[17] and may facilitate appropriate access to molecularly targeted therapy.

Limitations

This study included a small number of patients with rare diseases, and because of phenotypic heterogeneity and the invasiveness of tissue sampling, it was difficult to obtain the same number and type of specimens under identical conditions from all patients. In addition, because of the analytical detection limit, low-frequency variants below the analytical detection threshold may have been missed. Furthermore, the panel used in this study did not include some vascular-malformation-associated genes, including *TEK*; therefore, additional analysis using a broader gene panel or somatic exome/genome sequencing is required for negative cases.

Conclusions

In patients with coexisting overgrowth and vascular malformations, this study demonstrated that detection of the causal somatic variant differed according to tissue type. In *PIK3CA*-positive KTS, variants were consistently detected in overgrown skin/subcutaneous tissue and CM, whereas they were not detected in the corresponding VM specimens. In the mosaic RASopathy case, the same *KRAS* variant was detected in overgrowth tissue and another affected tissue without sampling the high-flow lesion itself. These findings suggest that, for the genetic diagnosis of vascular anomalies caused by somatic mosaicism, affected tissue should not simply be sampled indiscriminately; rather, an appropriate specimen should be selected by considering the suspected molecular background and tissue distribution of the variant together with both diagnostic value and procedural safety.

Abbreviations

cfDNA, cell-free DNA; CLVM, capillary-lymphatic-venous malformation; CM, capillary malformation; CT, computed tomography; CVM, capillary-venous malformation; FF, high-flow lesion group; IGV, Integrative Genomics Viewer; ISSVA, International Society for the Study of Vascular Anomalies; KTS, Klippel-Trenaunay syndrome; LIC, localized intravascular coagulopathy; LM, lymphatic malformation; MCAP, megalencephaly-capillary malformation syndrome; MRI, magnetic resonance imaging; NGS, next-generation sequencing; PI3K, phosphatidylinositol 3-kinase; PROS, *PIK3CA*-related overgrowth spectrum; VAF, variant allele fraction; VM, venous malformation.

Declarations

Ethics approval and consent to participate:

The study was approved by the Institutional Review Board of Tohoku University Hospital (No. 2025-1-541). Informed consent was obtained from all participants or their legal representatives. All procedures were conducted in accordance with the Declaration of Helsinki and its subsequent amendments.

Consent for publication:

Written informed consent for publication of anonymized clinical and genetic data was obtained from all participants or their parents/legal guardians, as appropriate.

Clinical Trial Registration: Not applicable.

Availability of data and materials:

Data are available from the corresponding author upon reasonable request, but not publicly available due to privacy/ethical restrictions.

Competing interests:

The authors declare that they have no competing interests.

Funding: This work was supported in part by JSPS KAKENHI Grant Numbers JP21K19436 (to Y.A.) and JP24K12819 (to A.S.).

Authors' contributions:

M.T., N.T., A.S., C.M., and Y.I. analyzed and interpreted the clinical presentation and diagnostic imaging data. T.N. and Y.A. performed the somatic variant analysis of the tissue biopsies.

M.T., T.N., and Y.A. were major contributors to writing the manuscript. All authors read and approved of the final manuscript.

Acknowledgements: We would like to express our sincere appreciation to Yoko Tateda for the valuable technical assistance.

Authors' information: Not applicable.

References

1. Goldenberg DC, Vikkula M, Penington A, Blei F, Kool LS, Wassef M, et al. Updated Classification of Vascular Anomalies. A living document from the International Society for the Study of Vascular Anomalies Classification Group. J Vasc Anom (Phila). 2025;6:e113. https://doi.org/10.1097/JOVA.0000000000000113.
2. Morin GM, Zerbib L, Kaltenbach S, Fraissenon A, Balducci E, Asnafi V, et al. PIK3CA-Related Disorders: From Disease Mechanism to Evidence-Based Treatments. Annu Rev Genomics Hum Genet. 2024;25:211–37. https://doi.org/10.1146/annurev-genom-121222-114518.
3. Madsen RR, Vanhaesebroeck B, Semple RK, Cancer-Associated. PIK3CA Mutations in Overgrowth Disorders. Trends Mol Med. 2018;24:856–70. https://doi.org/10.1016/j.molmed.2018.08.003.
4. Canaud G, Hammill AM, Adams D, Vikkula M, Keppler-Noreuil KM. A review of mechanisms of disease across PIK3CA-related disorders with vascular manifestations. Orphanet J Rare Dis. 2021;16:306. https://doi.org/10.1186/s13023-021-01929-8.
5. Keppler-Noreuil KM, Sapp JC, Lindhurst MJ, Parker VER, Blumhorst C, Darling T, et al. Clinical delineation and natural history of the PIK3CA-related overgrowth spectrum. Am J Med Genet A. 2014;164A:1713–33. https://doi.org/10.1002/ajmg.a.36552.
6. Mazoyer E, Enjolras O, Laurian C, Houdart E, Drouet L. Coagulation abnormalities associated with extensive venous malformations of the limbs: differentiation from Kasabach-Merritt syndrome. Clin Lab Haematol. 2002;24:243–51. https://doi.org/10.1046/j.1365-2257.2002.00447.x.
7. Canaud G, Lopez Gutierrez JC, Irvine AD, Vabres P, Hansford JR, Ankrah N, et al. Alpelisib for treatment of patients with PIK3CA-related overgrowth spectrum (PROS). Genet Med. 2023;25:100969. https://doi.org/10.1016/j.gim.2023.100969.
8. Sehgal SN. Sirolimus: its discovery, biological properties, and mechanism of action. Transplant Proc. 2003;35:7S-14S. https://doi.org/10.1016/s0041-1345(03)00211-2
9. Venot Q, Blanc T, Rabia SH, Berteloot L, Ladraa S, Duong J-P, et al. Targeted therapy in patients with PIK3CA-related overgrowth syndrome. Nature. 2018;558:540–6. https://doi.org/10.1038/s41586-018-0217-9.
10. Kim Y-M, Lee Y, Choi Y, Choi IH, Heo SH, Choi JM, et al. Clinical and genetic analyses of patients with lateralized overgrowth. BMC Med Genomics. 2022;15:206. https://doi.org/10.1186/s12920-022-01362-1.
11. Cottrell CE, Bender NR, Zimmermann MT, Heusel JW, Corliss M, Evenson MJ, et al. Somatic PIK3R1 variation as a cause of vascular malformations and overgrowth. Genet Med. 2021;23:1882–8. https://doi.org/10.1038/s41436-021-01211-z.

12. Couto JA, Huang AY, Konczyk DJ, Goss JA, Fishman SJ, Mulliken JB, et al. Somatic MAP2K1 Mutations Are Associated with Extracranial Arteriovenous Malformation. Am J Hum Genet. 2017;100:546–54. https://doi.org/10.1016/j.ajhg.2017.01.018.
13. Janardhan HP, Meng X, Dresser K, Hutchinson L, Trivedi CM. KRAS or BRAF mutations cause hepatic vascular cavernomas treatable with MAP2K-MAPK1 inhibition. J Exp Med. 2020;217:e20192205. https://doi.org/10.1084/jem.20192205.
14. Moog U, Felbor U, Has C, Zirn B. Disorders Caused by Genetic Mosaicism. Dtsch Arztebl Int. 2020;116:119–25. https://doi.org/10.3238/arztebl.2020.0119.
15. Kuentz P, St-Onge J, Duffourd Y, Courcet J-B, Carmignac V, Jouan T, et al. Molecular diagnosis of PIK3CA-related overgrowth spectrum (PROS) in 162 patients and recommendations for genetic testing. Genet Med. 2017;19:989–97. https://doi.org/10.1038/gim.2016.220.
16. Keppler-Noreuil KM, Rios JJ, Parker VER, Semple RK, Lindhurst MJ, Sapp JC, et al. PIK3CA-related overgrowth spectrum (PROS): diagnostic and testing eligibility criteria, differential diagnosis, and evaluation. Am J Med Genet A. 2015;167A:287–95. https://doi.org/10.1002/ajmg.a.36836.
17. Revencu N, Eijkelenboom A, Bracquemart C, Alhopuro P, Armstrong J, Baselga E, et al. Assessment of gene-disease associations and recommendations for genetic testing for somatic variants in vascular anomalies by VASCERN-VASCA. Orphanet J Rare Dis. 2024;19:213. https://doi.org/10.1186/s13023-024-03196-9.
18. Martínez MA, Muñoz-Ordoñez JR, Guzman JA, González-Zambrano MP, Gomez Castellanos DA, Estévez MF, et al. Transvenous biopsy of body cistyc lesions in a 32-year-old man with cloves syndrome and thrombocytopenia: a safe option for high bleeding risk patients. CVIR Endovasc. 2026;9:28. https://doi.org/10.1186/s42155-025-00541-2.
19. Goodwin S, McPherson JD, McCombie WR. Coming of age: ten years of next-generation sequencing technologies. Nat Rev Genet. 2016;17:333–51. https://doi.org/10.1038/nrg.2016.49.
20. Brandigi E, Torino G, Messina M, Molinaro F, Mazzei O, Matucci T, et al. Combined capillary-venous-lymphatic malformations without overgrowth in patients with Klippel-Trénaunay syndrome. J Vasc Surg Venous Lymphat Disord. 2018;6:230–6. https://doi.org/10.1016/j.jvsv.2017.09.011.
21. Sasaki Y, Ishikawa K, Hatanaka KC, Oyamada Y, Sakuhara Y, Shimizu T, et al. Targeted next-generation sequencing for detection of PIK3CA mutations in archival tissues from patients with Klippel–Trenaunay syndrome in an Asian population. Orphanet J Rare Dis. 2023;18:270. https://doi.org/10.1186/s13023-023-02893-1.
22. Nozawa A, Ozeki M, Niihori T, Suzui N, Miyazaki T, Aoki Y. A somatic activating KRAS variant identified in an affected lesion of a patient with Gorham-Stout disease. J Hum Genet. 2020;65:995–1001. https://doi.org/10.1038/s10038-020-0794-y.
23. Li H, Durbin R. Fast and accurate short read alignment with Burrows-Wheeler transform. Bioinformatics. 2009;25:1754–60. https://doi.org/10.1093/bioinformatics/btp324.
24. McKenna A, Hanna M, Banks E, Sivachenko A, Cibulskis K, Kernytsky A, et al. The Genome Analysis Toolkit: a MapReduce framework for analyzing next-generation DNA sequencing data. Genome Res.

2010;20:1297–303. https://doi.org/10.1101/gr.107524.110.

25. Wang K, Li M, Hakonarson H. ANNOVAR: functional annotation of genetic variants from high-throughput sequencing data. Nucleic Acids Res. 2010;38:e164. https://doi.org/10.1093/nar/gkq603.
26. Karczewski KJ, Francioli LC, Tiao G, Cummings BB, Alföldi J, Wang Q, et al. The mutational constraint spectrum quantified from variation in 141,456 humans. Nature. 2020;581:434–43. https://doi.org/10.1038/s41586-020-2308-7.
27. Higasa K, Miyake N, Yoshimura J, Okamura K, Niihori T, Saitsu H, et al. Human genetic variation database, a reference database of genetic variations in the Japanese population. J Hum Genet. 2016;61:547–53. https://doi.org/10.1038/jhg.2016.12.
28. Landrum MJ, Lee JM, Riley GR, Jang W, Rubinstein WS, Church DM, et al. ClinVar: public archive of relationships among sequence variation and human phenotype. Nucleic Acids Res. 2014;42:D980–985. https://doi.org/10.1093/nar/gkt1113.
29. Stenson PD, Mort M, Ball EV, Shaw K, Phillips A, Cooper DN. The Human Gene Mutation Database: building a comprehensive mutation repository for clinical and molecular genetics, diagnostic testing and personalized genomic medicine. Hum Genet. 2014;133:1–9. https://doi.org/10.1007/s00439-013-1358-4.
30. Robinson JT, Thorvaldsdóttir H, Winckler W, Guttman M, Lander ES, Getz G, et al. Integrative genomics viewer. Nat Biotechnol. 2011;29:24–6. https://doi.org/10.1038/nbt.1754.
31. Mirzaa G, Graham JM Jr, Keppler-Noreuil K, PIK3CA-Related Overgrowth Spectrum. 2013 Aug 15 [updated 2023 Apr 6]. In: Adam MP, Bick S, Mirzaa GM, Wallace SE, Amemiya A, editors. GeneReviews® [Internet]. Seattle (WA): University of Washington, Seattle; 1993 [cited 2026 Oct 4]. http://www.ncbi.nlm.nih.gov/books/NBK153722/
32. James A, Blumenstein L, Glaenzel U, Jin Y, Demailly A, Jakab A, et al. Absorption, distribution, metabolism, and excretion of [(14)C]BYL719 (alpelisib) in healthy male volunteers. Cancer Chemother Pharmacol. 2015;76:751–60. https://doi.org/10.1007/s00280-015-2842-4.
33. Morin G, Degrugillier-Chopinet C, Vincent M, Fraissenon A, Aubert H, Chapelle C, et al. Treatment of two infants with PIK3CA-related overgrowth spectrum by alpelisib. J Exp Med. 2022;219:e20212148. https://doi.org/10.1084/jem.20212148.
34. Dompmartin A, Acher A, Thibon P, Tourbach S, Hermans C, Deneys V, et al. Association of localized intravascular coagulopathy with venous malformations. Arch Dermatol. 2008;144:873–7. https://doi.org/10.1001/archderm.144.7.873.
35. Vanhaesebroeck B, Guillermet-Guibert J, Graupera M, Bilanges B. The emerging mechanisms of isoform-specific PI3K signalling. Nat Rev Mol Cell Biol. 2010;11:329–41. https://doi.org/10.1038/nrm2882.
36. Fruman DA, Chiu H, Hopkins BD, Bagrodia S, Cantley LC, Abraham RT. The PI3K Pathway in Human Disease. Cell. 2017;170:605–35. https://doi.org/10.1016/j.cell.2017.07.029.
37. Graupera M, Guillermet-Guibert J, Foukas LC, Phng L-K, Cain RJ, Salpekar A, et al. Angiogenesis selectively requires the p110alpha isoform of PI3K to control endothelial cell migration. Nature.

2008;453:662–6. https://doi.org/10.1038/nature06892.

38. Stanczuk L, Martinez-Corral I, Ulvmar MH, Zhang Y, Laviña B, Fruttiger M, et al. cKit Lineage Hemogenic Endothelium-Derived Cells Contribute to Mesenteric Lymphatic Vessels. Cell Rep. 2015;10:1708–21. https://doi.org/10.1016/j.celrep.2015.02.026.
39. Drake CJ, Little CD. Exogenous vascular endothelial growth factor induces malformed and hyperfused vessels during embryonic neovascularization. Proc Natl Acad Sci U S A. 1995;92:7657–61. https://doi.org/10.1073/pnas.92.17.7657.
40. Biesecker LG. Mosaic disorders and the Taxonomy of Human Disease. Genet Med. 2018;20:800–1. https://doi.org/10.1038/gim.2017.213.
41. Castillo SD, Baselga E, Graupera M. PIK3CA mutations in vascular malformations. Curr Opin Hematol. 2019;26:170–8. https://doi.org/10.1097/MOH.0000000000000496.
42. Boscolo E, Coma S, Luks VL, Greene AK, Klagsbrun M, Warman ML, et al. AKT hyper-phosphorylation associated with PI3K mutations in lymphatic endothelial cells from a patient with lymphatic malformation. Angiogenesis. 2015;18:151–62. https://doi.org/10.1007/s10456-014-9453-2.
43. Blesinger H, Kaulfuß S, Aung T, Schwoch S, Prantl L, Rößler J, et al. PIK3CA mutations are specifically localized to lymphatic endothelial cells of lymphatic malformations. PLoS ONE. 2018;13:e0200343. https://doi.org/10.1371/journal.pone.0200343.
44. Le Cras TD, Goines J, Lakes N, Pastura P, Hammill AM, Adams DM, et al. Constitutively active PIK3CA mutations are expressed by lymphatic and vascular endothelial cells in capillary lymphatic venous malformation. Angiogenesis. 2020;23:425–42. https://doi.org/10.1007/s10456-020-09722-0.
45. Tooming M, Mertsina P, Kahre T, Teek R, Vainumäe I, Lilles S, et al. Uncovering somatic mosaic variants of PIK3CA-related overgrowth disorders - three cases with different clinical presentations. Front Genet. 2025;15:1484651. https://doi.org/10.3389/fgene.2024.1484651.
46. Castillo SD, Tzouanacou E, Zaw-Thin M, Berenjeno IM, Parker VER, Chivite I, et al. Somatic activating mutations in Pik3ca cause sporadic venous malformations in mice and humans. Sci Transl Med. 2016;8:332ra43. https://doi.org/10.1126/scitranslmed.aad9982.
47. He Y, Lin J, Li Y, Zeng W, Li Y. Cellular heterogeneity and tissue specificity in venous malformations: Implications for pathogenesis and targeted therapies. Prog Biophys Mol Biol. 2025;197:34–47. https://doi.org/10.1016/j.pbiomolbio.2025.06.002.
48. Colmenero I, Knöpfel N. Venous Malformations in Childhood: Clinical, Histopathological and Genetics Update. Dermatopathol (Basel). 2021;8:477–93. https://doi.org/10.3390/dermatopathology8040050.
49. Chen H, Sun B, Liu H, Gao W, Qiu Y, Hua C, et al. Delineation of the phenotypes and genotypes of PIK3CA-related overgrowth spectrum in East asians. Mol Genet Genomics. 2024;299:66. https://doi.org/10.1007/s00438-024-02159-w.
50. Du Z, Liu J-L, You Y-H, Wang L-Z, He J, Zheng J-W, et al. Genetic landscape of common venous malformations in the head and neck. J Vasc Surg Venous Lymphat Disord. 2021;9:1007–e10167.

https://doi.org/10.1016/j.jvsv.2020.11.016.

51. Groesser L, Herschberger E, Ruetten A, Ruivenkamp C, Lopriore E, Zutt M, et al. Postzygotic HRAS and KRAS mutations cause nevus sebaceous and Schimmelpenning syndrome. Nat Genet. 2012;44:783–7. https://doi.org/10.1038/ng.2316.
52. Aoki Y, Niihori T, Narumi Y, Kure S, Matsubara Y. The RAS/MAPK syndromes: novel roles of the RAS pathway in human genetic disorders. Hum Mutat. 2008;29:992–1006. https://doi.org/10.1002/humu.20748.
53. Al-Olabi L, Polubothu S, Dowsett K, Andrews KA, Stadnik P, Joseph AP, et al. Mosaic RAS/MAPK variants cause sporadic vascular malformations which respond to targeted therapy. J Clin Invest. 2018;128:1496–508. https://doi.org/10.1172/JCI98589.
54. Chang CA, Perrier R, Kurek KC, Estrada-Veras J, Lehman A, Yip S, et al. Novel findings and expansion of phenotype in a mosaic RASopathy caused by somatic KRAS variants. Am J Med Genet A. 2021;185:2829–45. https://doi.org/10.1002/ajmg.a.62356.
55. Diociaiuti A, Rotunno R, Pisaneschi E, Cesario C, Carnevale C, Condorelli AG, et al. Clinical and Molecular Spectrum of Sporadic Vascular Malformations: A Single-Center Study. Biomedicines. 2022;10:1460. https://doi.org/10.3390/biomedicines10061460.
56. Slack JC, Bründler M-A, Chang CA, Perrier R, Lafay-Cousin L, Kurek KC. Bilateral Nephroblastic Tumors and a Complex Renal Vascular Anomaly in a Patient With a Mosaic RASopathy: Novel Histopathologic Features and Molecular Insights. Pediatr Dev Pathol. 2021;24:235–40. https://doi.org/10.1177/1093526620986502.
57. Schmidt VF, Wieland I, Wohlgemuth WA, Ricke J, Wildgruber M, Zenker M. Mosaic RASopathy due to KRAS variant G12D with segmental overgrowth and associated peripheral vascular malformations. Am J Med Genet A. 2021;185:3122–8. https://doi.org/10.1002/ajmg.a.62386.
58. Mussa A, Turchiano A, Cardaropoli S, Coppo P, Pantaleo A, Bagnulo R, et al. Lateralized overgrowth with vascular malformation caused by a somatic PTPN11 pathogenic variant: Another piece added to the puzzle of mosaic RASopathies. Genes Chromosomes Cancer. 2022;61:689–95. https://doi.org/10.1002/gcc.23086.

Figures

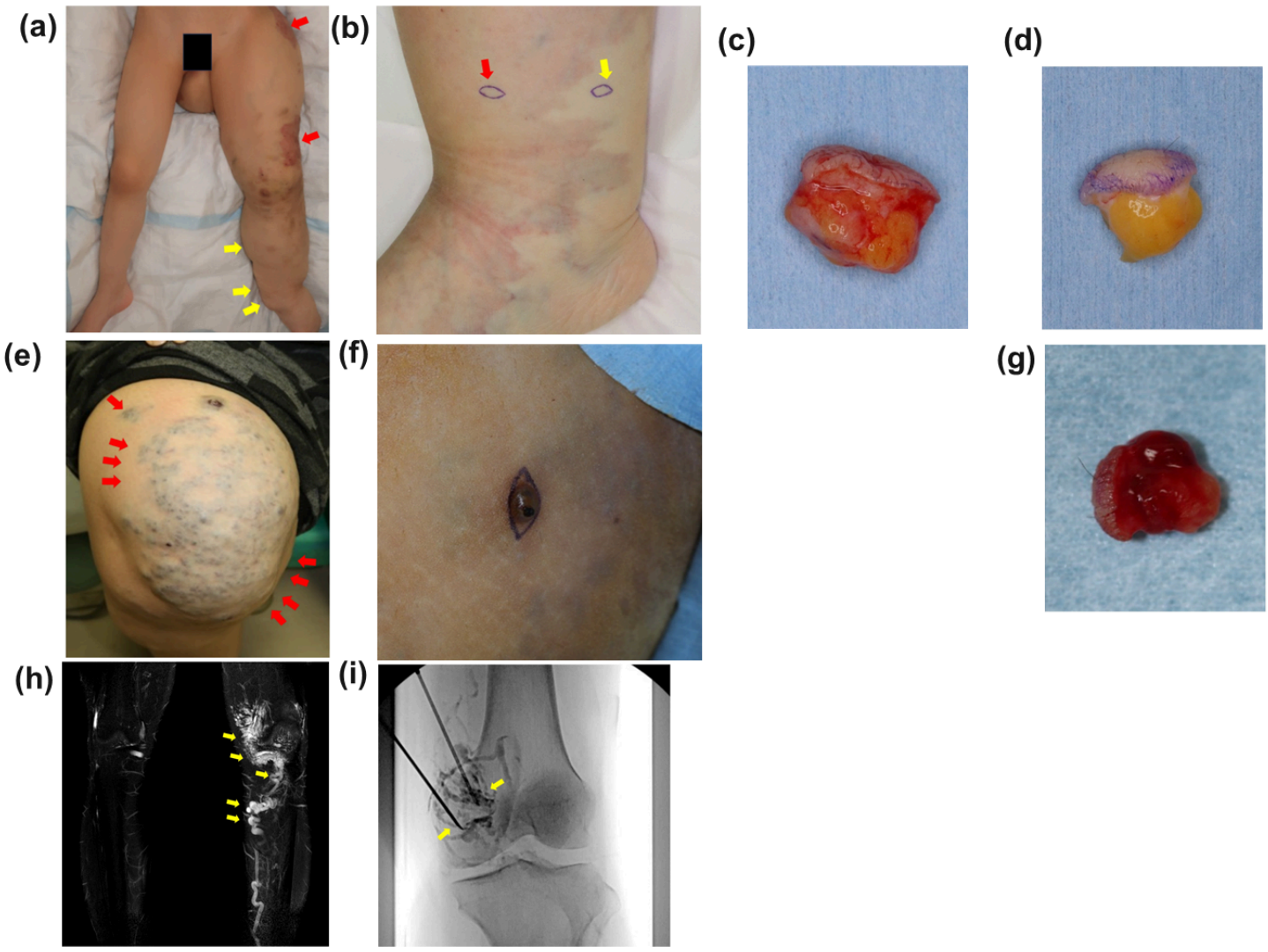


Figure 1

Multi-tissue sampling protocol

(a) Red arrow: The capillary malformation, characterized by mottled erythematous patches, was selected as the sampling site.

Yellow arrow: A skin-colored area within the region of overgrowth, with no superficial lesions such as erythematous patches, was selected as the sampling site.

(b) The marked sampling sites for the capillary malformation (red arrow) and overgrown tissue (yellow arrow) are shown.

(c) A tissue specimen obtained from the capillary malformation lesion is shown. A tissue specimen including the skin and subcutaneous tissue was obtained to a depth of approximately 1 cm.

(d) A tissue specimen obtained from the area of tissue overgrowth is shown.

(e) Red arrow: Superficial venous malformation: Venous malformation lesions visible as bluish discoloration through the skin were selected as sampling sites.

(f) A superficial venous malformation lesion is shown.

(g) A tissue specimen was obtained from the subcutaneous lesion contiguous with the superficial venous malformation, to a depth of approximately 1 cm.

(h) Yellow arrow: Deep venous malformation: Tissue samples from venous malformations located in the deep subcutaneous tissue were obtained by multiple needle biopsies.

(i) Yellow arrow: Needle biopsy procedure. The lesion was visualized under fluoroscopic guidance following contrast injection, and tissue samples were obtained through multiple needle biopsies performed at several sites within the lesion.

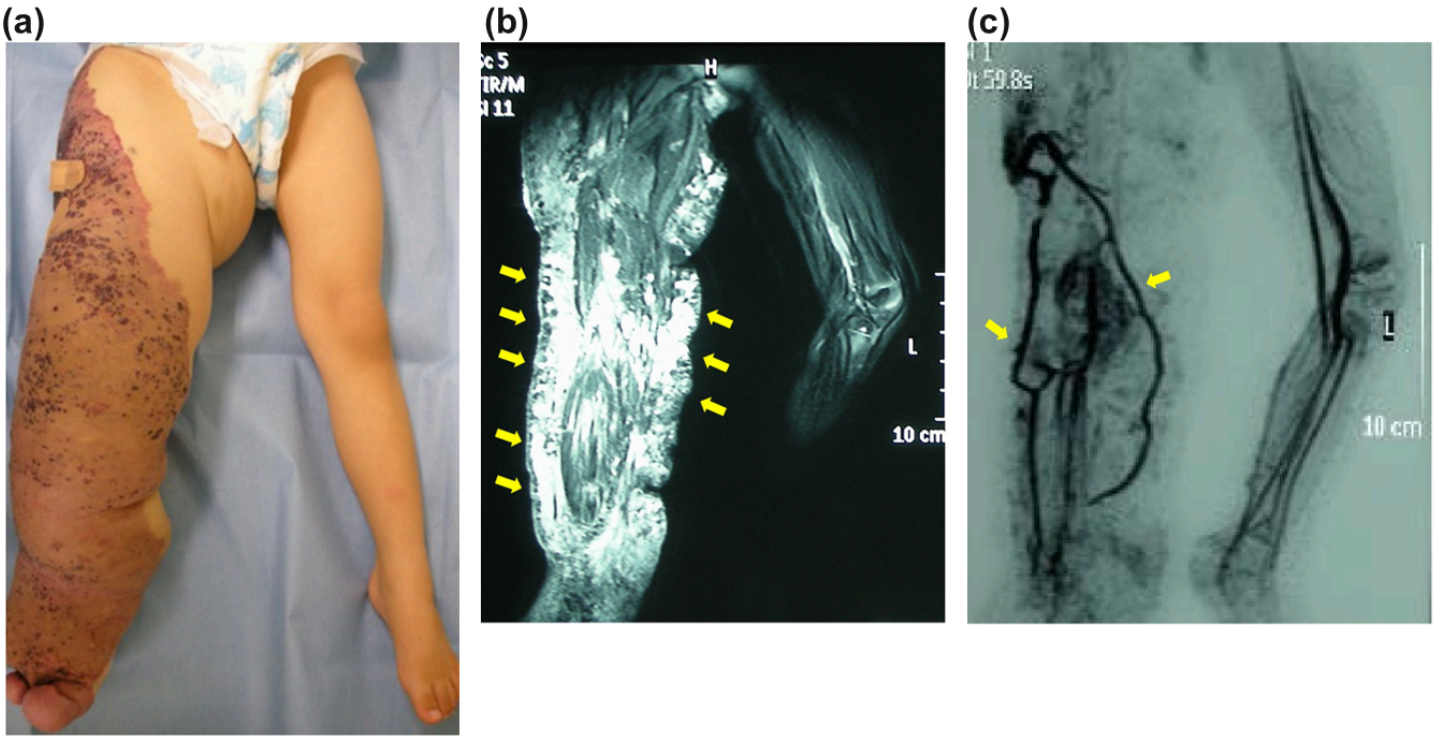


Figure 2

KTS1 CLVM type

(a) Soft-tissue overgrowth of the right lower extremity and leg-length discrepancy are observed, together with extensive capillary malformations and superficial lymphatic malformations.

(b) Yellow arrows: T2-weighted MR images demonstrate extensive lymphatic-venous malformations involving the subcutaneous soft tissues of the right lower extremity.

(c) Yellow arrows: Contrast-enhanced MR images demonstrate markedly dilated and tortuous anomalous veins in the right lower extremity.

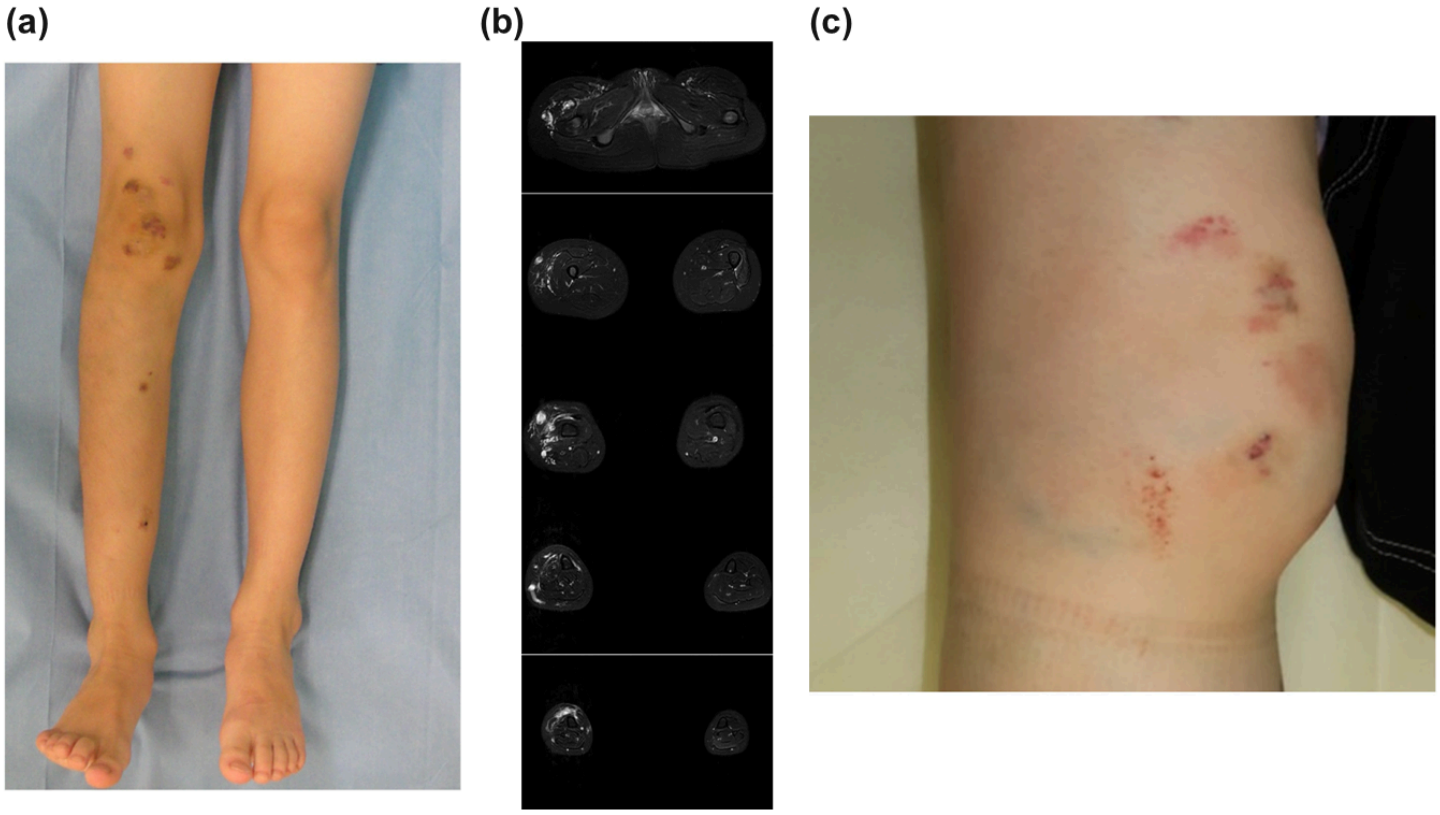


Figure 3

KTS9 CVM type

(a) Mild soft-tissue overgrowth of the right lower extremity, leg-length discrepancy, and venous dilatation are present. Patchy erythematous lesions are scattered.

(b) Fat-suppressed T2-weighted MR images demonstrate enlargement of the affected limb compared with the contralateral unaffected limb, with multiple venous malformations and dilated veins in the subcutaneous tissues and muscles.

(c) Patchy capillary malformations are observed predominantly around the right knee.

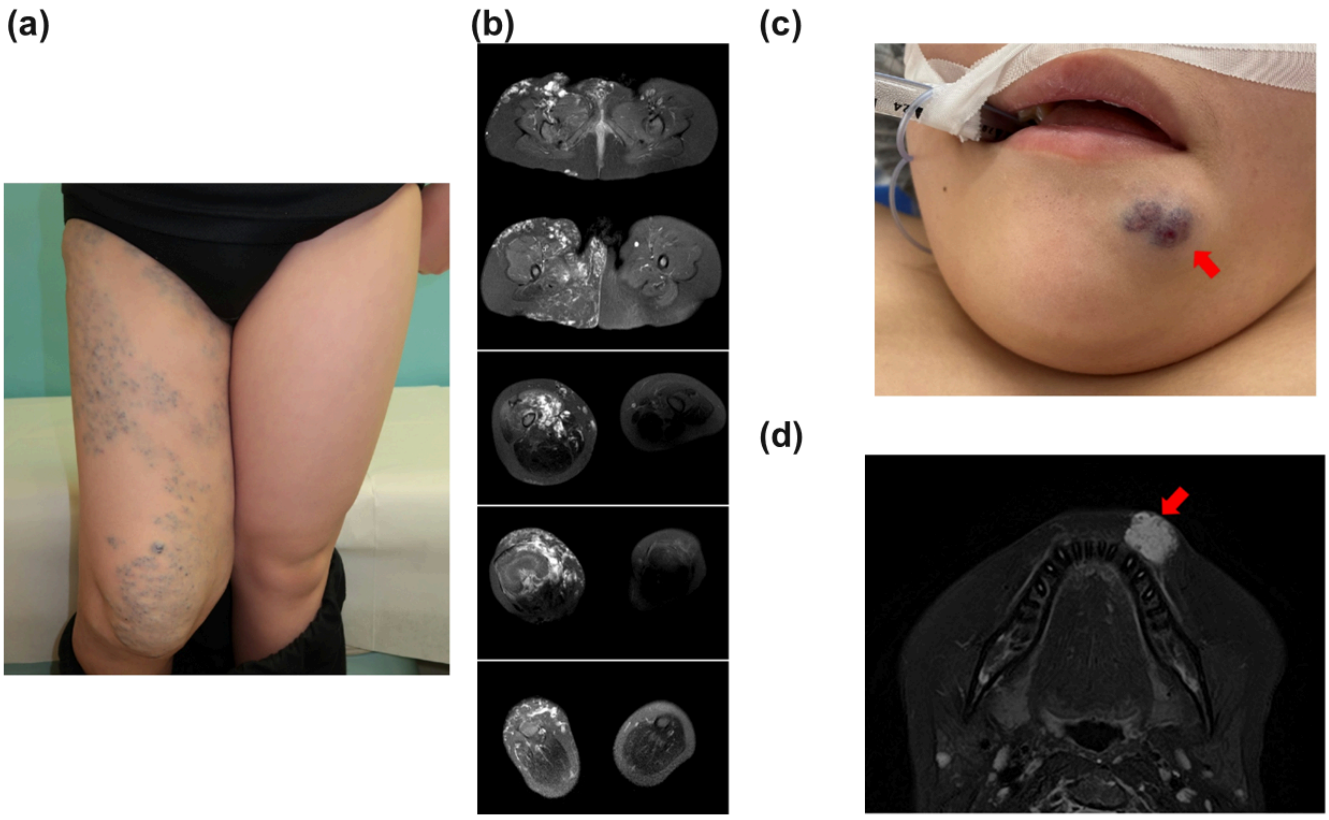


Figure 4

VM1

(a) Soft-tissue overgrowth of the right lower extremity and leg-length discrepancy are present, with extensive superficial venous malformations extending from the lumbar region to the thigh and knee.

(b) Fat-suppressed T2-weighted MR images demonstrate enlargement of the affected limb compared with the contralateral unaffected limb, with multiple venous malformations involving the skin, subcutaneous tissues, and deep soft tissues.

(c) Red arrow: Venous malformation lesion localized to the left mandibular region

(d) Red arrow: A venous malformation in the subcutaneous tissue of the left mandibular region on fat-suppressed T2-weighted MR images.

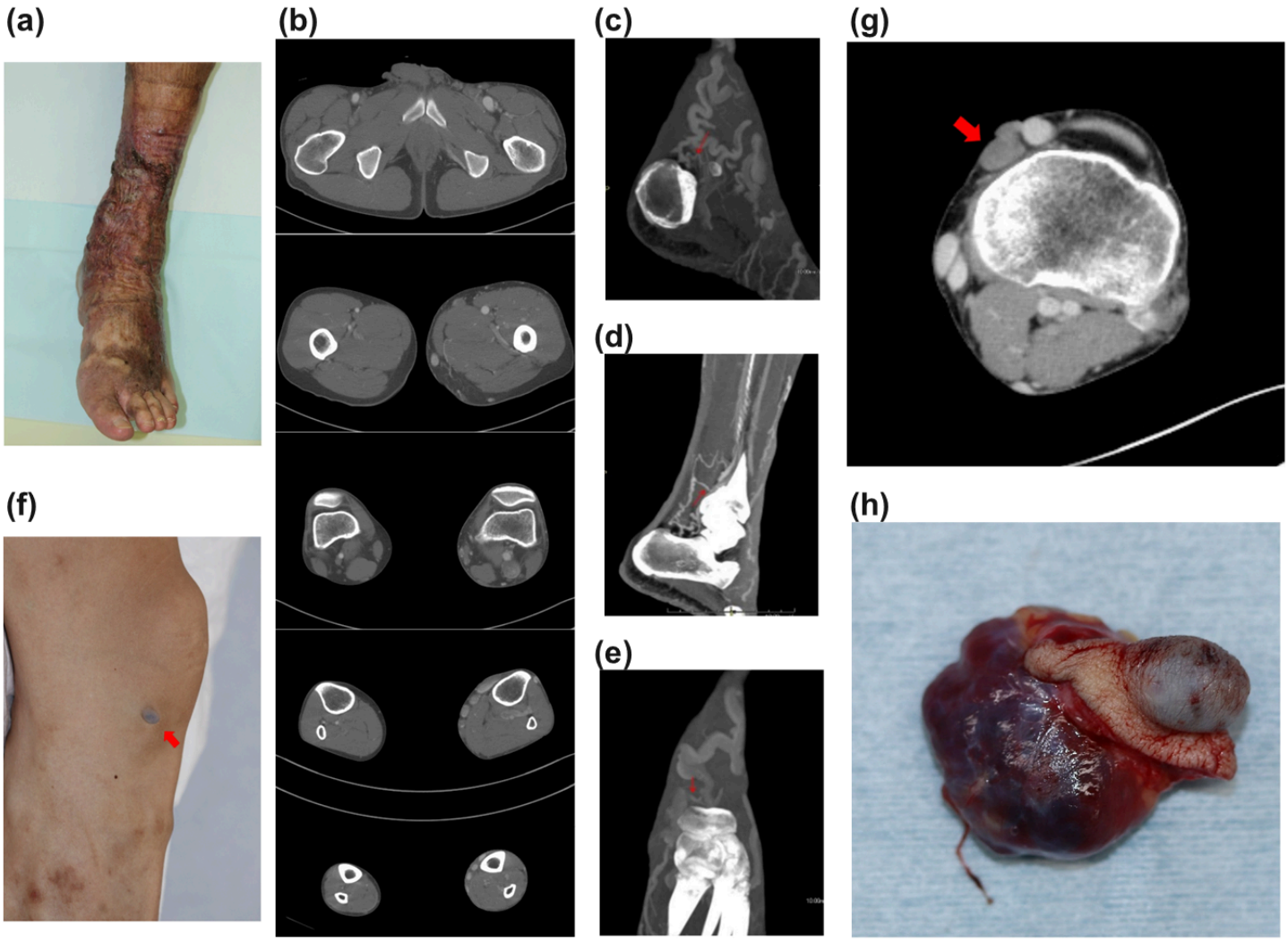


Figure 5

Fast-flow case

(a) A cutaneous plaque with erythematous discoloration, dryness, and dilated superficial veins is observed on the left lower extremity.

(b) Contrast-enhanced CT image of the left lower extremity. Soft-tissue overgrowth is observed compared with the contralateral side. Dilated superficial veins are visualized during the arterial phase, suggesting the presence of arteriovenous shunting.

(c) Red arrow: The posterior tibial artery communicates with dilated, tortuous veins at the ankle.

(d) Red arrow: The peroneal artery communicates with a dilated vein.

(e) Red arrow: The dorsalis pedis artery communicates with a dilated vein.

(f) A nodular vascular lesion is observed in the left knee region, which bleeds during the application and removal of compression stockings.

(g) Contrast-enhanced CT image showing an enhancing nodular vascular lesion.

(h) The nodular vascular lesion was excised together with the overlying skin lesion.

Supplementary Files

This is a list of supplementary files associated with this preprint. Click to download.

- Table34.docx
- Table12.docx